Journal of Biomechanics 103 (2020) 109640

Contents lists available at ScienceDirect

Journal of Biomechanics

journal homepage: www.elsevier.com/locate/jbiomech
www.JBiomech.com

Fluid-structure interaction modeling of lactating breast

Jamasp Azarnoosh, Fatemeh Hassanipour *

Department of Mechanical Engineering, The University of Texas at Dallas, 800 W. Campbell Road, Richardson, TX 75080, USA

ARTICLE INFO

Article history:
Accepted 13 January 2020

Keywords:
Breastfeeding
Oral cavity abnormality
Computational fluid dynamics
Finite element method
Bio-transport

ABSTRACT

There are two theories for the dynamics of milk expression by the infant. One hypothesis is that milk expression is due to the negative pressure applied by the infant sucking; the alternative hypothesis is that the tongue movement and squeezing of nipple/areola due to mouthing is responsible for the extraction of milk from the nipple. In this study, 3-D two-way Fluid-Structure Interaction (FSI) simulations are conducted to investigate the factors that play the primary role in expressing milk from the nipple. The models include the solid deformation and periodic motion of the tongue and jaw movement. To obtain the boundary conditions, ultrasound images of the oral cavity and motion of the tongue movement during breastfeeding are extracted in parallel to the intra-oral vacuum pressure. The numerical results are cross-validated with clinical data. The results show that, while vacuum pressure plays an important role in the amount of milk removal, the tongue/jaw movement is essential for facilitating this procedure by decreasing the shear stress within the main duct in the nipple. The developed model can contribute to a better understanding of breastfeeding complications due to infant or breast abnormalities and for the design of medical devices such as breast pumps and artificial teats.

1. Introduction

Breastfeeding is a dynamic process that includes oscillating vacuum pressure on the surface of the nipple and the rhythmic infant tongue and jaw movement, leading to milk expression from the nipple. There are two proposed theories regarding the main factors influencing milk removal during breastfeeding. One theory emphasizes the infant's jaw movement and peristaltic motion of the tongue on the inferior surface of the nipple/areola. The other theory emphasizes the negative intra-oral pressure by the infant. However, the precise mechanism of breastfeeding and the extraction of milk from the nipple is still not conclusively established.

Computational studies have been performed on many biological organs such as human pulmonary tract (Azarnoosh et al., 2020; Gemci et al., 2008; Imai et al., 2012), blood vessels (Tse et al., 2011; Valen-Sendstad et al., 2013; Drewe et al., 2017), brain (Kurtcuoglu et al., 2007; Moore et al., 2006), and heart (King et al., 1996; Nobili et al., 2008). These studies have found relevance in the diagnosis and treatment of diseases as well as the development of various bio-medical devices and surgical procedures. Computational modeling of the lactating breast, however, has not received the same attention. A better understanding of the physical factors that contribute to milk removal in the lactating breast can lead to the treatment of many breastfeeding problems and the development of biomedical devices.

Several attempts have been made over the last decades to understand the factors that play an important role in milk removal from the nipple during the lactation process. The early study on lactation was performed by Basch (1893) who developed an artificial breast to experimentally study feeding behavior. He reported the infant's jaw movement as the key factor for the milk expression while later studies referred to intra-oral pressure to draw milk from the nipple (Kron and Litt, 1971; Pfaundler, 1899).

Kron and Litt (1971) developed a technique for the simultaneous control and measurement of pressure and flow during nutritive suckling. This study emphasized on intra-oral pressure only and ignored the influence of infant's mouthing.

Various methodologies were proposed to investigate and understand the breastfeeding mechanism. A mathematical model of breastfeeding was developed by Zoppou et al. (1997) based on quasi-linear poroelastic theory to compare milk extraction between infant breastfeeding and the use of a breast pump. The model showed the critical role of tongue movement, leading to a high volume of expressed milk.

Geddes et al. (2008) used ultrasound images to study the relationship between the tongue movement, negative vacuum pres-

* Corresponding author at: Department of Mechanical Engineering, The University of Texas at Dallas, 800 W. Campbell Road, Richardson, TX 75080-3021, USA.
E-mail address: fatemeh@utdallas.edu (F. Hassanipour).

https://doi.org/10.1016/j.jbiomech.2020.109640
0021-9290/

sure by the infant's mouth, and milk ejection from the breast. They observed that milk expression would increase as the intra-oral vacuum pressure increases with the simultaneous downward movement of the tongue.

In a recent study by Alatalo et al. (2020) applied thin-film pressure sensors, and vacuum pressure transducers simultaneously along with the ultrasound imaging to map the dynamics of breast-infant interaction during breastfeeding. They obtained a range of positive (compression) and negative (vacuum) pressure created by the infant oral cavity during breastfeeding.

Mortazavi et al. (2015) used mathematical modeling to study milk flow transport in the breast ductal system. They reported that for the minimum flow resistance, there is an optimal range of branch generations leading to the easiest milk flow. In another study by the same authors, a numerical simulation of lactation within a six-generation ductal system was performed with the assumption of the ductal system as a rigid body (Mortazavi et al., 2017). They showed that the maximum intra-oral vacuum pressure was not relevant to the highest milk expression from the nipple. Elad et al. (2014) simulated the mechanics of breastfeeding considering a symmetric two-generation ductal model with a periodic pressure cycling. Their observation from ultrasound images and simulation emphasized the importance of vacuum pressure in milk expression during breastfeeding.

In the present study, a 3-D computational model is developed for simulations of breastfeeding mechanism. The model includes the interaction of the lactating breast and the infant oral cavity. To study the factors involved with the milk expression from the lactating breast, four separate cases with the corresponding boundary conditions are studied.

2. Methods

2.1. Geometry and meshing method

In this study, the breasts of five lactating women are scanned using a Polhemus FastSCAN 3-D scanning device (Alatalo et al., 2020). The geometry is developed in Solidworks by averaging the dimensions of the scanned women's breasts as shown in Fig. 1. The breast geometry is modeled with a hemispherical shape of 60 mm radius which is comprised of the nipple, areola, and a single non-planar axisymmetric ductal system (lobe). Based on the data, the initial free nipple length and width of 10.5 mm and 16 mm are considered in the model, respectively. The anatomy of the breast shows that the human breast includes 5 to 9 lobes (Geddes, 2007). Also, a previous study by Mortazavi et al. (2015)shows that the optimum bifurcation level in the lactating human breast is approximately 25. However, due to the computational cost and available resources, this work is limited to a single lobe with a maximum of four bifurcation levels. The angle of bifurcations is assumed to be 20° based on the observation of real ductal system images by Baum et al. (2008). This assumption also allows the inclusion of 5 to 9 lobe models with up to seven bifurcations for future studies.

An unstructured mesh is generated for the entire model using ANSYS Meshing. Two types of meshes are generated for the fluid (milk ducts) and solid domain (the breast, mouth, and tongue) as outlined in Table 2. The volume mesh of the fluid domain is generated using inflation-layer meshing to generate an off-wall spacing. This methodology leads to the extrusion of regular layers of prism elements from boundaries to adequately capture near-wall flow physics. The cross-sectional view in Fig. 1 shows the generated mesh in the first bifurcation. For mesh convergence study of the solid domain, the critical regions where the breast geometry is expected to have contact with the infant's mouth are refined, including the nipple, areola, oral cavity surfaces and superior surface of the tongue.

2.2. Material properties

A homogeneous incompressible hyperelastic material is considered for the breast model, including the nipple and the areola. The hyperelastic model of adipose tissue, which behaves in accordance with the Mooney-Rivlin model, is applied based on the *ex vivo* breast tissue measurements by Samani and Plewes (2004). The Mooney-Rivlin material model for five parameters in the form of the strain energy potential function (W) is defined as:

$$W = C_{10}(\bar{I}_1 - 3) + C_{01}(\bar{I}_2 - 3) + C_{11}(\bar{I}_1 - 3)(\bar{I}_2 - 3) + C_{20}(\bar{I}_1 - 3)^2 + C_{02}(\bar{I}_2 - 3)^2 + \frac{1}{d}(J - 1)^2 \quad (1)$$

where $\bar{I}_1$ is the first deviatoric strain invariant, $\bar{I}_2$ is the second deviatoric strain invariant, J is determinant of the elastic deformation gradient, d is the material incompressibility parameter, and C_{10}, C_{01}, C_{11}, C_{20} and C_{02} are material constants, characterizing the deviatoric deformation of the material, and assigned as adipose tissue with the values of 310 pa, 300 pa, 2250 pa, 3800 pa, and 4720 pa, respectively (Samani and Plewes, 2004). The material property of the infant's tongue is not available in the literature. There are several studies on adult's tongue mechanical properties with application to speech therapy (Cheng et al., 2011; Li et al., 2017). However, these data cannot be used for the purpose of this study because the infant's tongue shows more softness and flexibility. Therefore, the infant's tongue is assumed to behave similarly to the breast tissue.

The Neo-Hookean material model is assumed with an initial shear modulus of 70,000 Pa (Elad et al., 2014) for the infant's tongue. The Neo-Hookean form of strain energy potential W is defined as:

$$W = \frac{\mu_{ism}}{2}(\bar{I}_1 - 3) + \frac{1}{d}(J - 1)^2 \quad (2)$$

where μ_{ism} is the initial shear modulus of the material.

Milk is assumed to be a Newtonian fluid with a constant density (ρ) of 1030 kg/m^3 and averaged viscosity (μ) of 0.02758 kg/m-s, respectively (Mortazavi et al., 2015).

2.3. Simulation methods

The current FSI simulations are based on the partitioned approach by coupling a flow solver (ANSYS Fluent) and a structural solver (ANSYS Mechanical APDL), where the fluid and solid domains are treated as independent models with separate meshes. The system of equations in both domains is solved separately and sequentially for each time interval. The number of iterations per coupling step is case-dependent to achieve a converged solution. The maximum coupling iteration is set to 50 for the four-generation lobe model case.

The fluid analysis is performed in ANSYS Fluent and governed by the continuity and Navier-Stokes equations using the pressure-based scheme. The fluid is laminar incompressible due to the low Reynolds number calculated within the main duct, by considering the hydraulic diameter of the duct cross-section. The discretization approach to solve these equations is finite volume. The implicit pressure-based scheme (SIMPLE) is selected, and a second-order accurate time stepping and discretization scheme is applied (Patankar, 1980). Criterion-type is considered to be absolute for computational fluid dynamics simulation (CFD) simulations and the convergence criteria of the continuity and momentum equations are set to be 10^{-6} with maximum 50–80 sub-iterations depending on the case of study.

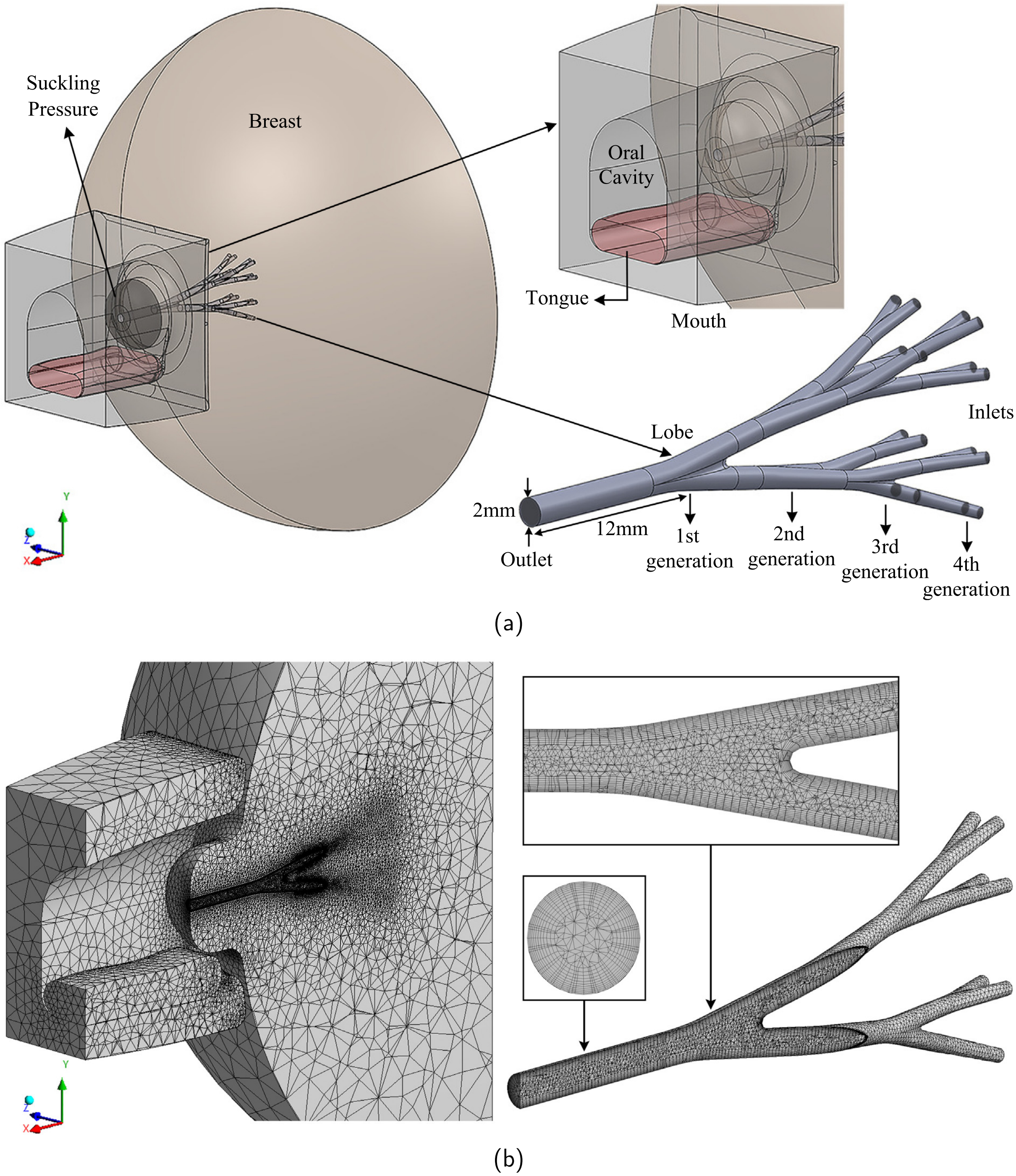

Fig. 1. (a) The 3-D geometry model including the infant's mouth, tongue, breast, and a four-generation ductal system (lobe), and (b) sagittal cross-sectional mesh view of the breast model and lobe.

The structural analysis is considered to be transient in order to determine the dynamic response of a structure under time-dependent loads. The analysis is based on the finite elements by solving the equations using a Lagrangian formulation.

The convergence study is carried out to assess the appropriate time step size and mesh. Three time steps of 0.01 s, 0.02 s, and 0.04 s are selected and also two types of meshes are considered (see Table 2). Simulation of the selected time steps and mesh sizes reveals only a 2% error in the accumulation of the milk.

2.4. Boundary conditions

The FSI simulation of breastfeeding requires two sets of boundary conditions: (1) the vacuum (suckling) pressure on the nipple, (2) the deformation of the nipple and areola due to the dynamic interaction of the infant's mouth and breast.

The vacuum pressure data is collected using a tube pressure transducer attached to the breast Alatalo et al. (2020). The profile of the measured vacuum pressure shows an approximately constant sinusoidal waveform. Therefore, to reduce the computational solution time, the simulations are limited to two cycles corresponding to 1.5 s (from 2 to 3.5 s) as shown in Fig. 2. This intra-oral vacuum pressure profile is applied at the outlet boundary of the lobe in the fluid domain along with the total gauge pressure of zero at the inlets (lobules).

Parallel with pressure measurement, an endocavity convex transducer placed under the infant's chin produces ultrasound images from a cross-section of the oral cavity and time-dependent motion of the wave-like tongue movement during breastfeeding (see Fig. 3). These ultrasound images track the displacement of the upper and lower jaws to measure the nipple width and length (Alatalo et al., 2020). The nipple shape in two instantaneous times of ultrasound images when the tongue is up (compression is maximum and vacuum pressure is minimum) and when the tongue is down (compression is minimum and vacuum pressure is maximum) are shown in Fig. 3a and b, respectively. Changes in the nipple dimension in the ultrasound video are processed and analyzed using MATLAB. A self-programmed measurement system is utilized to obtain the average dimensions of the nipple length and width. An in-depth discussion of this procedure is outlined in Alatalo et al. (2020). Based on the observation from the ultrasound images, the boundary conditions on the solid domain are applied in the following three steps:

1. Latching on procedure which involves the infant displacement of the mouth and compression of the breast surface within one second. This displacement is assumed to be 5 mm toward the breast during the one second time interval. The infant's jaw had full contact with the breast at the end of this phase.
2. Elongation of the nipple during the next one second phase due to the mouth's closure on the surface of the nipple-areola. Vertical displacement of the hard palate is assumed to be 6.5 mm in the opposite y-direction whereas the lower jaw displaced upward for 4.5 mm. The displacement of the upper and the lower jaws make the vertical opening of the mouth to become 11 mm, which matches the ultrasound images observations.
3. The final step is the periodic movement of the tongue during the nutritive suckling. Based on ultrasound images, the upper palate is set to be fixed in the simulation while the lower jaw moves periodically up and down along the y-direction. Simultaneously, the vacuum pressure from the clinical data is applied on the surface of the nipple in the solid domain as well as the outlet of the lobe in the fluid domain.

3. Results and discussion

3.1. Cross validation with clinical data

The variation of the nipple and infant's mouth dimensions from the simulation are compared with ultrasound images for validation purposes (see Video 1). Fig. 4 shows the variation of nipple/mouth dimensions in x and y directions from the latching moment until the end of two periodic suck cycles. To obtain the nipple elongation in the x-direction, two probe points are considered as shown in a cross-sectional view of the breast in Fig. 4a. Point-1 and point-2 are placed on the tip of the nipple and base of the nipple, respectively. This figure shows the displacement of points-1, point-2, and elongation of the nipple, which is measured based on the two selected points. The origin of the coordinate system is considered to be fixed at the initial location of point-2 ($t = 0$ s).

As shown in Fig. 4, the latch-on occurs within two seconds of the simulation. During the first second, the mouth movement toward the breast causes no deformation on the nipple. Following the latch-on process, compression of the nipple/areola by the infant's mouth causes the nipple teat elongation to 16.2 mm at 2 s as shown in Fig. 4a. The Intra-oral vacuum pressure and the periodic motion of the tongue cause the nipple to reach its maximum length of 18.5 mm. The simulation model, as well as the ultrasound images, show that the length of the nipple becomes approximately twice its initial free length.

The same procedure is used for measuring the nipple and mouth width deformation in the y-direction by considering four probe points as shown in Fig. 4b. Point-3 and point-4 are on the hard palate and the superior surface of the nipple, respectively. These points are selected in the locations where they overlap during the suckling process. Similarly, point-4 and point-5 are placed on the tip of the tongue and the inferior surface of the nipple, respectively. The displacement of these points from the reference (point-2) during 3.5 s of the simulation is measured and plotted in Fig. 4b. The measurements reveal that the nipple reaches its minimum width of 11 mm before nutritive suckling begins. As the tongue moves down to its lowest position, the nipple width becomes 13.3 mm. However, a small gap between the nipple and the upper jaw is observed at the maximum mouth opening where the superior surface of the nipple detaches from the upper jaw for a short period of time while the tongue still has full contact with the

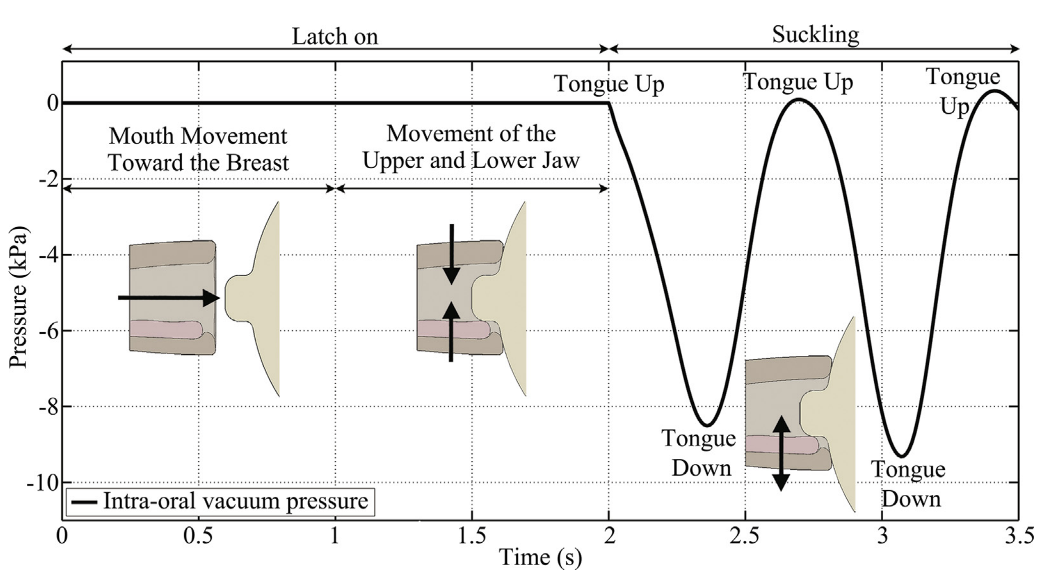

Fig. 2. Intra-oral vacuum pressure profile during nutritive breastfeeding and the boundary conditions applied to the infant's mouth in the various stages.

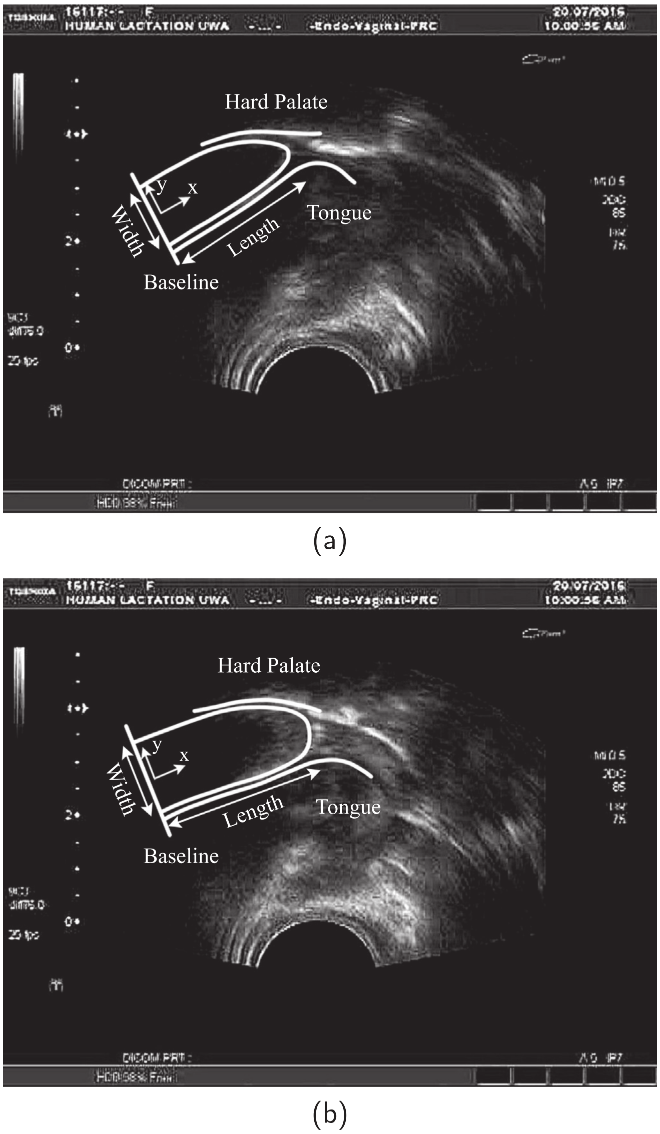

Fig. 3. Infant's mouth and nipple boundary movement via ultrasound images. (a) Tongue up (maximum compression, minimum vacuum pressure), and (b) tongue down (minimum compression, maximum vacuum pressure).

areola. This demonstrates the significance of the tongue motion on nipple deformation other than the upper jaw.

Fig. 5 shows the comparison of deformation from the simulation model and ultrasound images for both changes in mouth/nipple width (ΔW) and nipple elongation (ΔL) during the suckling time interval ($2.0 \leqslant t(s) \leqslant 3.5$). As observed, the tongue, nipple and jaw displacements are in good agreement with the clinical data. The average nipple elongation (ΔL) is approximately 2.5 mm and the average variation of the mouth/nipple, (ΔW) is approximately 2.7 mm during nutritive suckling.

3.2. Vacuum pressure vs. compression

To study the effect of vacuum pressure versus compression pressure on milk removal, separate simulations are conducted by applying the four cases of boundary conditions as outlined in Table 1. The results for the volumetric milk flow rate at the outlet of the nipple tip is obtained for each case during the suckling time interval as shown in Fig. 6a.

The results in Case-1 indicate a significantly higher volumetric flow rate for about three times larger than Case-3 and Case-4, which is due to the variation in the volume of the fluid domain in deformed cases compared to the rigid body (Case-1). The comparison of the results with clinical data is performed by providing the calculated milk accumulation as shown in Fig. 6b. Case-1 has the highest accumulated milk volume of 0.8 ml per cycle.

The deformation of the breast model in Case-3 causes a significant drop in the milk expression to 0.3 ml per cycle. The infant's mouthing also shows its effect on the expressed milk, which is mainly related to the compression of the ductal system. The results for Case-2 show a very small amount of milk expression, which reveals the importance of vacuum pressure for milk removal. The compression only in Case-2 results in 0.016 ml per cycle milk expression.

The importance of mouthing/compression by the infant's tongue can be gauged by comparing Case-3 (vacuum pressure only, e.g. breast pumps) and Case-4 (natural suckling including both vacuum pressure and compression). However, the results of the milk flow rate for both cases show small changes, meaning the vacuum pressure plays an important role in milk removal from the breast. The main reason for the slight difference is the reduction of the cross-sectional area of the duct by the compression.

The impact of the infant's mouthing is more pronounced when the tongue is in its highest position. As the vacuum pressure increases and the tongue moves downward (at $t = 2.36$ s or 3.08 s) the duct opens and provides easier milk expression. The upward motion of the tongue compresses the duct (at $t = 2.72$ s or 3.4 s) and causes a shift in the trend of volumetric flow rate compared to Case-3. This phenomenon has been also observed in Case-2. In this case, the infant's mouth compresses the nipple, and a small amount of milk discharges from the nipple tip. At this point, the mouth starts to open and causes a small amount of reverse flow and sudden drop in the milk flow.

The previous clinical investigations showed that the milk expression varies from one infant to another or days of feeding. The range of milk accumulation from different female breasts is 0.1 to 1.3 ml per cycle based on the studies by Bowen-Jones et al. (1982) and Mortazavi et al. (2017). The accumulated milk in natural suckling (Case-4) is 0.28 ml per cycle, which is within a reasonable range based on the previous clinical investigations.

3.3. Wall shear stress

As the results show, there is a small difference in terms of overall milk accumulation between Case-3 and Case-4. Therefore, we emphasize the flow characteristic and the shear stress inside the ductal system to reveal the role of mouthing and jaw movement on the lactation procedure.

Distribution of WSS varies in time due to the intra-oral vacuum pressure and compression by jaw movement (see Video 2). Two critical time marks are selected where the tongue is up, compression is maximum and vacuum pressure is minimum ($t = 2.72$ s), and where the tongue is down, compression is minimum and vacuum pressure is maximum ($t = 3.08$ s) as shown in Fig. 7. The value of WSS is limited to 10^{-6} Pa and 10^{-4} Pa when the vacuum pressure is minimum and maximum, respectively. The distribution of WSS at the maximum vacuum pressure is two orders of magnitude higher compared to minimum vacuum pressure, meaning that the vacuum pressure is the main reason for increasing the shear stress through the ducts. The results indicate that the first junction and nipple tip are two regions that the most variation of the WSS occurs during suckling. The region with high WSS in the first level of bifurcation is mainly due to the compression of the jaw in that region.

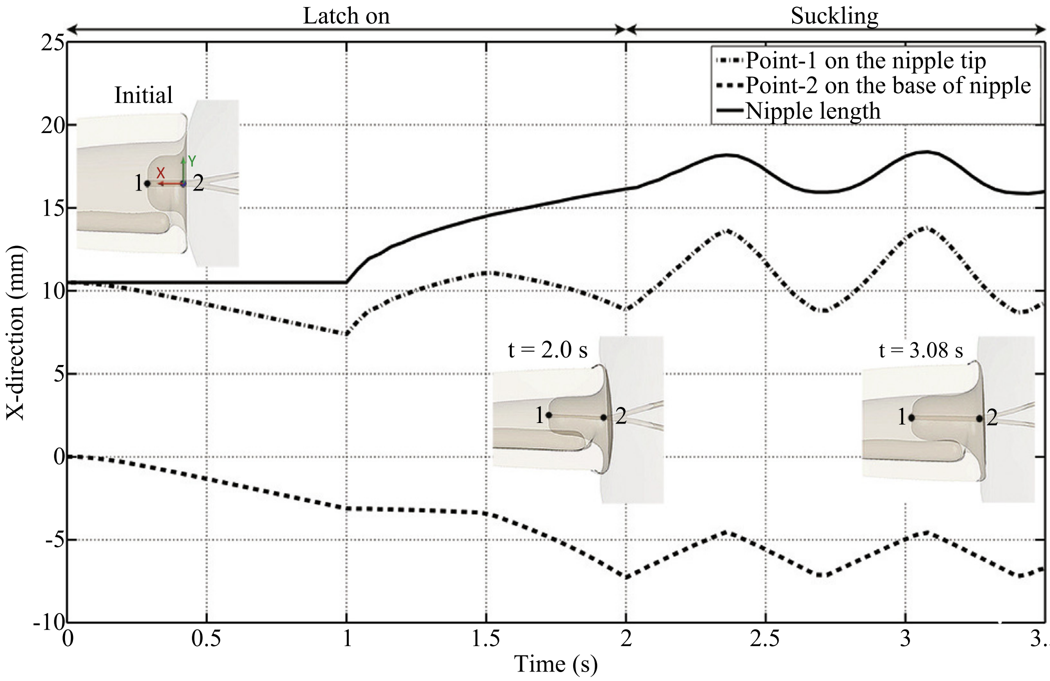

(a)

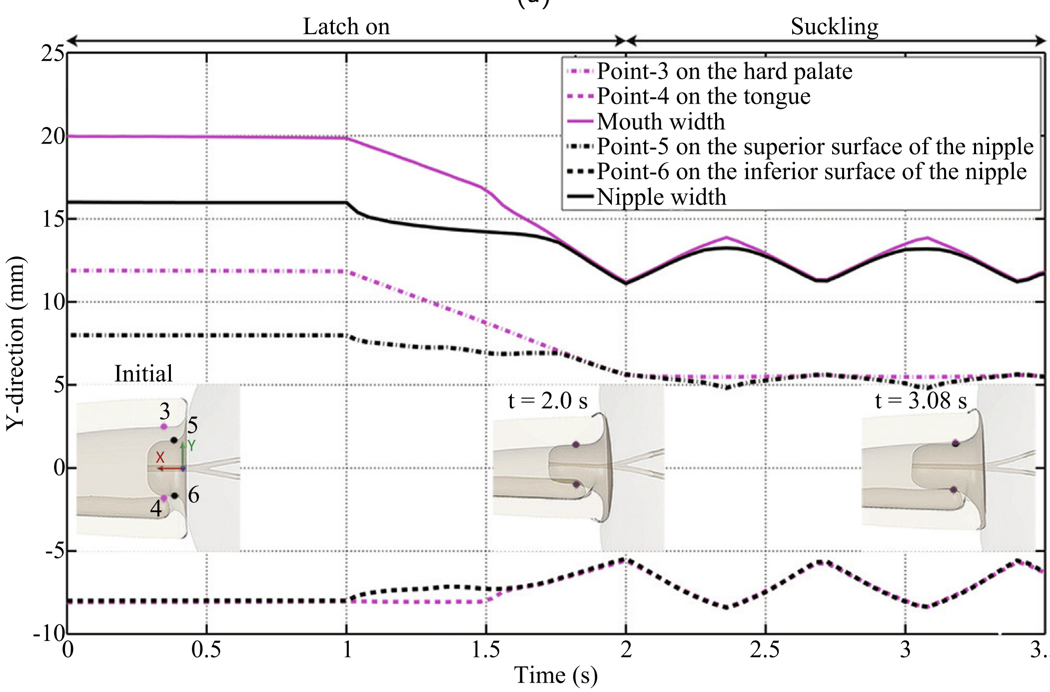

(b)

Fig. 4. (a) Nipple length deformation in x-direction, and (b) nipple and mouth width deformation in y-direction (Video 1).

The deformation of nipple causes the duct cross-sectional area variation, leading to local velocity changes. Therefore, the local WSS values shown in Fig. 7 are based on the velocity at that specific spot i.e. tip of the nipple. As shown in Fig. 8, the local velocity magnitude on the tip of the nipple is larger in case-3 compared with case-4. This leads to a smaller local WSS near the nipple tip in case-4 compared to case-3. The comparison between Case-3 and Case-4, for both minimum and maximum vacuum pressure, shows that adding compression pressure by jaw leads to low shear stress occurring near the tip of the nipple. This can emphasize the importance of mouthing and periodic motion on tongue and jaw movement for facilitating the milk removal.

3.4. Milk flow streamline

Observations reveal that the flow field is laminar, showing no circulation or chaotic flow in all cases (see Video 3). The flow characteristic implies that the milk flow behaves as the quasi-steady Hagen-Poiseuille flow within the ducts. Fig. 8 illustrates the velocity contour and streamlines for all four cases at an instantaneous

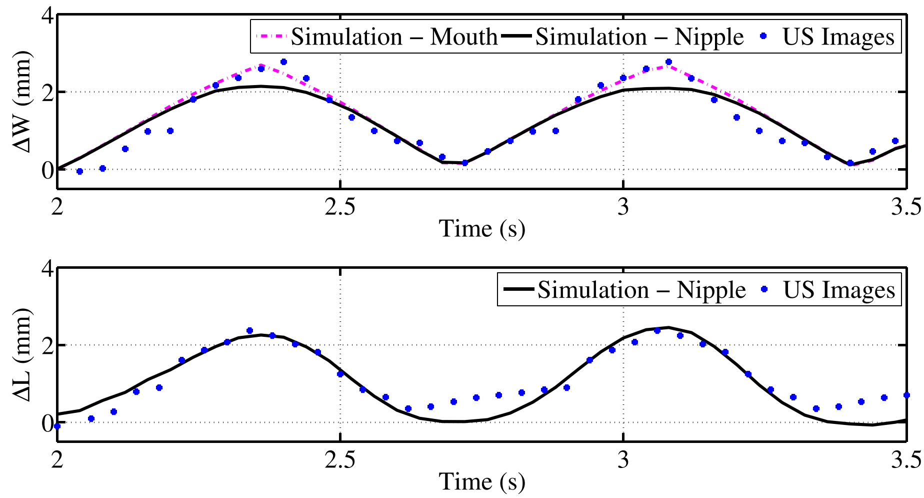

Fig. 5. Mouth/nipple width deformation (ΔW) and nipple elongation (ΔL), simulation vs. ultrasound images.

Table 1
The cases with the boundary conditions considered in the study.

Case No.	Boundary Conditions	
Case-1	Vacuum pressure only and the rigid duct body with no deformation	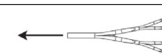
Case-2	Compression (mouthing) exerted by infant's jaws on the breast surface	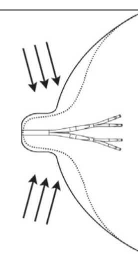
Case-3	Nipple elongation due to the vacuum pressure (e.g. breast pumps)	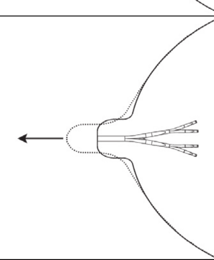
Case-4	Vacuum pressure along with the deformation of nipple and areola due the compression by infant's jaws on the breast (natural suckling)	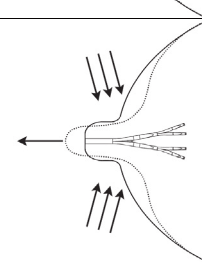

time t = 3.08 s. The velocity values in Case-2 are expected to be nearly zero. However, it is observed that the compression by the infant causes a small amount of milk expression. For the other cases that the vacuum pressure is applied, a high-velocity flow streamline is observed within the first bifurcation.

The magnitude of velocity reduces significantly through each successive generation. This observation is consistent in all cases. The factor that distinguishes these cases is the deformation of the breast by imposing various boundary conditions. Applying only suckling causes the ductal system to significantly stretch in Case-3. This elongation mainly impacts the shape of the duct in the zeroth generation (the region from the nipple tip to the first bifurcation level) and consequently results in different velocity behavior compared to Case-1. Including the deformation exerted by mouthing

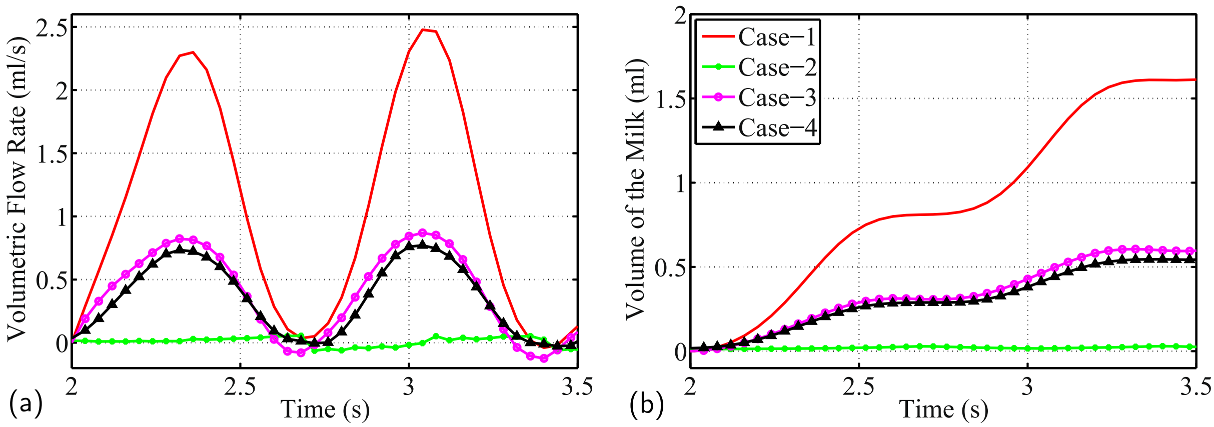

Fig. 6. (a) The volumetric flow rate, and (b) accumulated milk for all four cases of the four-generation lobe model within 1.5 s (from 2.0 s to 3.5 s).

Table 2
The number of nodes and volume elementsof the solid and fluid domains, and the CPU time of the cases.

	Lobe Models							
Mesh Type	One-Generation		Two-Generation		Three-Generation		Four-Generation	
	Nodes	Elements	Nodes	Elements	Nodes	Elements	Nodes	Elements
Solid (Coarse)	60 k	317 k	85 k	454 k	133 k	722 k	221 k	1213 k
Solid (Fine)	152 k	801 k	180 k	952 k	228 k	1,218 k	275 k	1499 k
Fluid (Coarse)	34 k	91 k	79 k	212 k	186 k	510 k	390 k	1090 k
Fluid (Fine)	53 k	123 k	106 k	244 k	351 k	844 k	711 k	1759 k
	Lobe Models							
	One-Generation		Two-Generation		Three-Generation		Four-Generation	
Case-1 (Coarse)	5 (mins)		12 (mins)		22 (mins)		40 (mins)	
Case-1 (Fine)	8 (mins)		16 (mins)		28 (mins)		50 (mins)	
Case-2 (Coarse)	2		2.5		4		6	
Case-2 (Fine)	2.5		3		5		7	
Case-3 (Coarse)	1		2		3		4	
Case-3 (Fine)	1.5		2.5		4		5	
Case-4 (Coarse)	2		2.5		4		6	
Case-4 (Fine)	2.5		3		5		7	

also shows changes in the velocity field causing a slight reduction in the maximum flow velocity compared with Case-3.

The sagittal cross-sectional view of the velocity contour is provided in Fig. 8 to show the velocity behavior in the first bifurcation where most critical changes occur. The zeroth generation in Case-3 shows a slightly higher velocity magnitude compared to natural suckling. The maximum Reynolds number of 70 is observed in the main duct for Case-4. The flow behaves differently in the junction of Case-3 showing a low-velocity magnitude compared to Case-4. This is due to the stretching of the ductal system causing the reduction of the bifurcation angle. In contrast, the junction in Case-4 experiences more deformation due to the compression by the infant's mouth and consequently causes high-velocity flow in this area.

The results indicate that the deformation of the ductal system by the infant's mouth leads to prominent changes in the milk flow characteristics as shown between a rigid body and deformed cases. This implies that the two-way FSI simulation is critical in the numerical modeling of breastfeeding.

3.5. Limitations and future perspectives

The numerical simulation of breastfeeding is a challenging problem due to the complexity of the human breast anatomy, the mechanism of the suckling by the infant, and also the milk fluid properties. For instance, consideration of a breast model with a realistic number of bifurcation levels may lead to new insights. Also, more accurate material properties of the breast tissue, infant's mouth, and tongue are missing in the literature, which requires a further multi-disciplinary study. Another limitation is the assumption of zero total gauge pressure at the inlet boundary condition. This is due to the lack of the previous studies on measuring the pressure values of alveoli. Also, the non-Newtonian behavior of milk studied previously by the authors (Alatalo and Hassanipour, 2016; Azarnoosh and Hassanipour, 2019), in conjunction with the solid deformation modeling, adds to the cost and complexity of the numerical simulation.

4. Conclusion

This study presents a fluid-structure interaction modeling to investigate the biomechanics of breastfeeding. The clinical data, including the vacuum pressure and nipple deformation, were obtained via *in vivo* measurements and incorporated in the numerical simulation.

This study indicates that both the vacuum pressure and the deformation of the nipple contribute to milk expression. Vacuum pressure plays a key role in the amount of milk extraction from the nipple, while the positive pressure exerted by the jaw movement on the areola facilitates milk removal by opening and closing the main duct in the nipple and lowering the shear stress inside the main duct. Furthermore, milk flow behavior inside the ductal

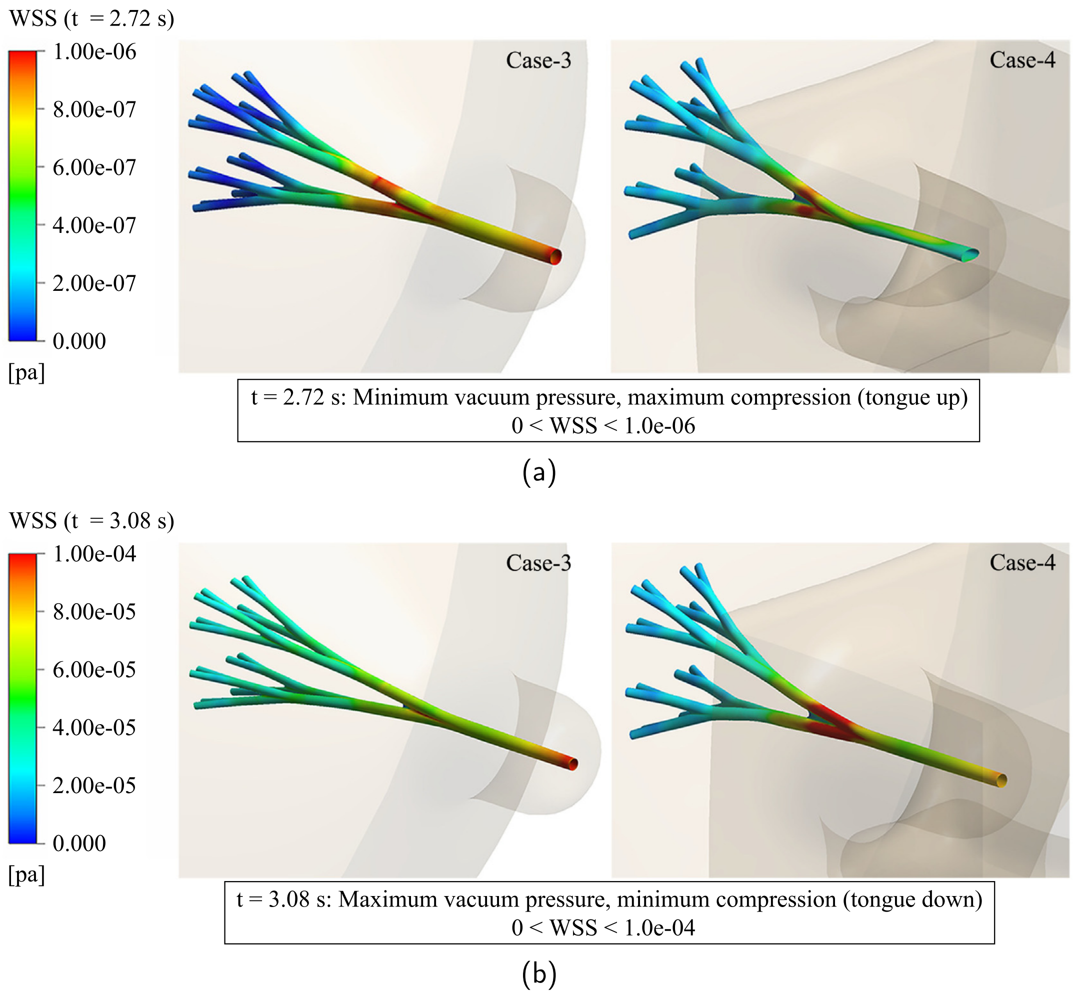

Fig. 7. Comparison of WSS distribution at (a) minimum, and (b) maximum vacuum pressure (Video 2).

system, which is hard to measure *in vivo*, was studied via simulation. The deformation of the breast during suckling, leading to the volume variation of the milk ducts, has a significant effect on the transient behavior of milk flow velocity and the resulting wall shear stress through the ducts. This was established by comparing flow patterns and velocities under a variety of boundary conditions.

Declaration of Competing Interest

The authors declare that they have no known competing financial interests or personal relationships that could have appeared to influence the work reported in this paper.

Acknowledgement

This material is based on work supported by the National Science Foundation Grants #1454334, and #1614350.

Appendix A. Effect of bifurcation levels on the CFD modeling

The bifurcated ductal system in this study includes up to four generations. To assess the impact of bifurcation level (n) on the results of the cases outlined in Table 1, similar simulations are performed for three other generation models (i.e. one- to three-generation lobe model). All generation models reveal similar observations of breast deformation and milk flow behavior that are discussed for the four-generation model. Therefore, the number of bifurcation level is independent of the study cases. However, the bifurcation level has an impact on the amount of milk expression from the nipple. A linear reduction of the milk accumulation with respect to the bifurcation level is observed as shown in Fig. A.1. In other words, as the generation level increases the amount of accumulated milk decreases. The value of milk expressed for the one-generation model is 0.36 ml/cycle. The expressed milk linearly decreases to 0.28 ml/cycle for the four-generation model. This observation is consistent with the previous study by Mortazavi et al. (2015) whom developed a mathematical model that represents the optimal bifurcation level of 25 for minimum milk flow resistance. However, the FSI analysis of 25-generation model cannot be performed due to the limitation of the current computational resources. Since no critical changes in the deformation and the milk flow characteristic are observed in the comparison of the first four-generation models, we believe that further generation levels do not affect the results of the milk expression significantly.

Appendix B. Governing equations

In the numerical simulation of the breastfeeding, two-way FSI analysis is performed using the partitioned approach where the physical systems are decomposed into partitions and the solution is obtained separately in each solver. In the current study, a flow solver (ANSYS Fluent) and a structural solver (ANSYS Mechanical APDL) are coupled.

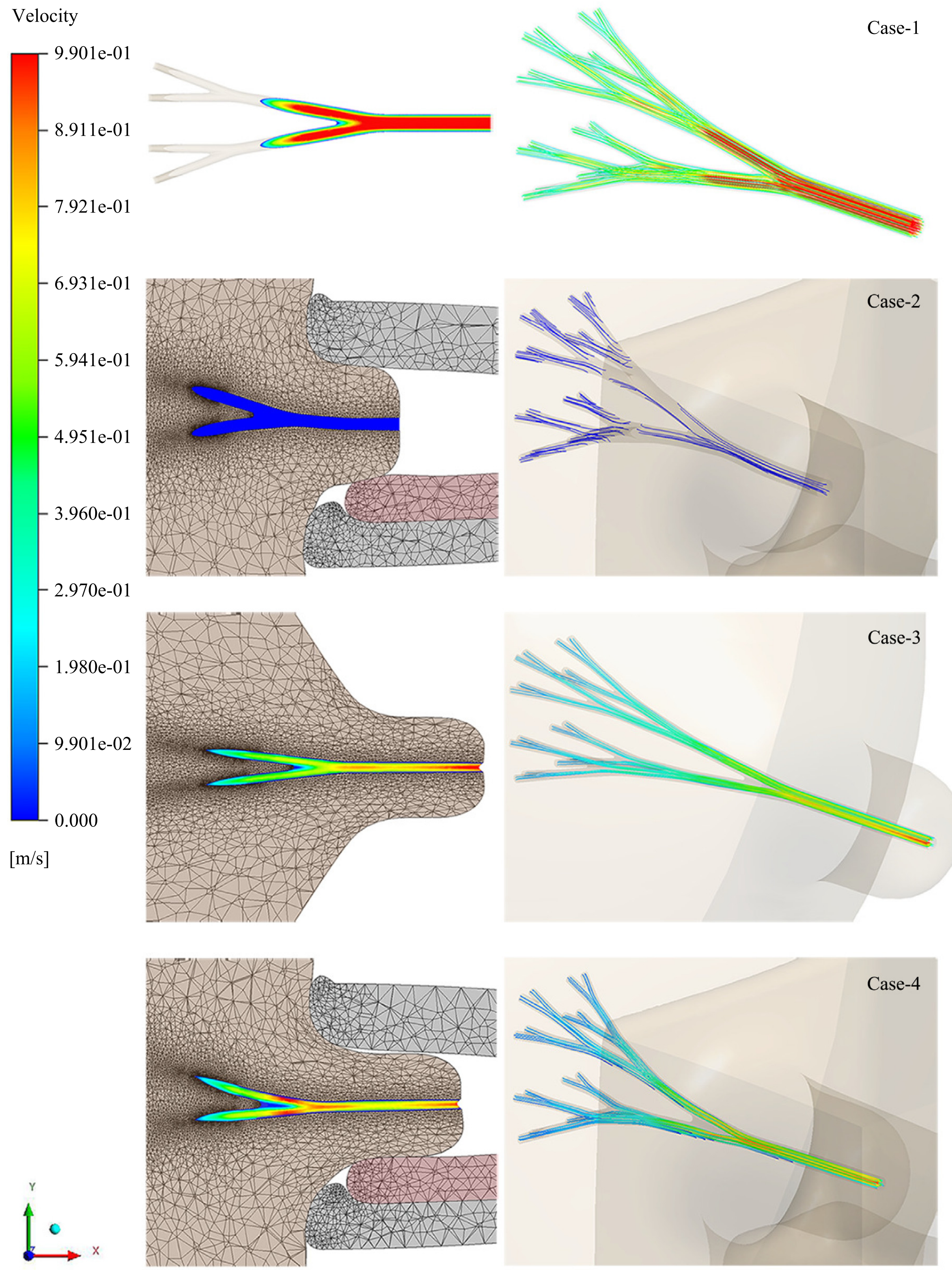

Fig. 8. Streamlines and velocity magnitude contour at 3.08 s where the milk flow rate is maximum (maximum vacuum pressure) for cases 1, 3 and 4, minimum compression for cases 2 and 4 (see Video 3).

The fluid is laminar incompressible flow due to the low Reynolds number within the ducts. The fluid analysis is conducted by solving the continuity and Navier-Stokes equations using the pressure-based scheme. The discretization approach is finite volume to solve the fluid governing equations, defined as:

$$\nabla \cdot \overrightarrow{U} = 0 \tag{B.1}$$

$$\rho \frac{\partial \overrightarrow{U}}{\partial t} + \rho \left(\overrightarrow{U} \cdot \nabla \right) \overrightarrow{U} = -\nabla P + \mu \nabla^2 \overrightarrow{U} \tag{B.2}$$

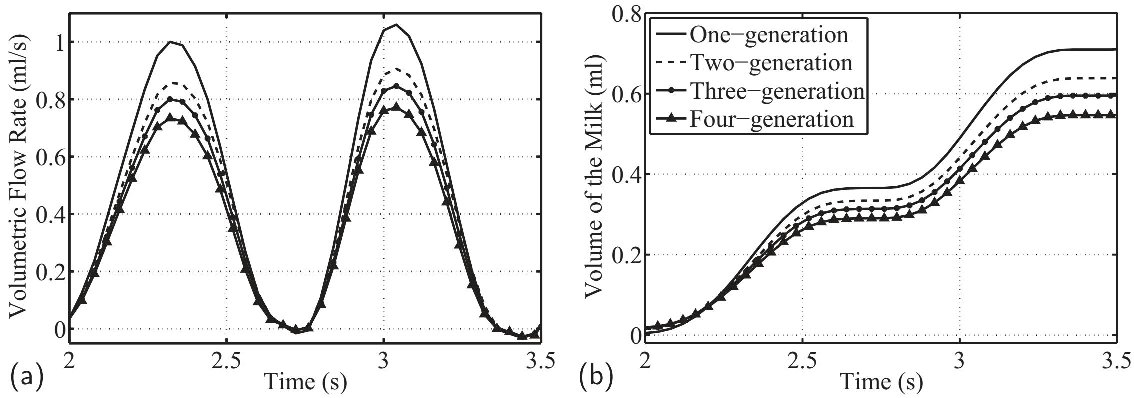

Fig. A.1. (a) The volumetric flow rate, and (b) accumulated milk for all four bifurcation lobe models within 1.5 s (from 2.0 s to 3.5 s) in the natural suckling (Case-4).

where $\overrightarrow{U}$ and P are the velocity and pressure of the fluid domain, respectively. The transient analysis is performed for the solid domain to determine the dynamic response of the structure under time-dependent loads. The governing equation of the structural domain is based on the equation of motion, defined as:

$$[M]\{\ddot{u}_{(t)}\} + [C]\{\dot{u}_{(t)}\} + [K]\{u_{(t)}\} = \{F_{(t)}\} \tag{B.3}$$

where M, C, and K are the structural mass, damping, and stiffness matrices, respectively. The vectors $u_{(t)}$ and $F_{(t)}$ are the nodal displacement and applied forces, respectively. The Newmark time integration method was used, which is implicit transient analysis. The analysis was based on finite elements using the Lagrangian formulation. The hyperelastic material properties of the structure point to the fact that the problem is nonlinear. Therefore, the internal load behaves nonlinearly to the nodal displacement.

The FSI analysis starts with the solution of the fluid domain. The values of forces (pressure and shear forces) are calculated in the fluid domain using the Eqs. (B.1) and (B.2), and transmitted to the solid via the fluid-solid interface (Γ). The Eq. (B.3) calculates the displacements in the solid domain and transfer back the data to the fluid field. The fluid-solid interface is the transmission conditions between the fluid and structure as defined in Eq. (B.4).

$$\sigma_s \cdot \hat{n} = \sigma_f \cdot \hat{n} \tag{B.4}$$

where $\hat{n}$ is outward unit normal vector and σ_s and σ_f are the fluid and solid stress tensor, respectively. The velocity of the fluid is equal to the wall velocity. The relationship between fluid velocity ($\overrightarrow{U}$) and displacement of the solid ($u_{(x,t)}$) at the interface is defined in Eq. (B.5).

$$\overrightarrow{U} = \dot{u}_{(x,t)} = \frac{\partial u}{\partial t} \tag{B.5}$$

The Eqs. (B.4) and (B.5) are the matching conditions at the fluid-solid interface. The fluid domain deforms after achieving the converge solution in structural solver with the expression Eq. (B.6).

$$\frac{\partial u}{\partial t} = \frac{\partial u_m}{\partial t} \tag{B.6}$$

where u_m is the deformation of the fluid mesh.

The coupling interface regions are defined in the System Coupling component system to transfer force and displacement data within the fluid-solid interface. This procedure continues until a converged solution is achieved. Since the problem is nonlinear and unstable, the stabilization factor is used to damp the transmitted data via the interface. This helps the difficulties in the solution convergence. The number of iterations per coupling step is dependent on the value of the stabilization factor. A bigger stabilization factor requires more coupling iterations.

Appendix C. Supplementary material

Supplementary data associated with this article can be found, in the online version, at https://doi.org/10.1016/j.jbiomech.2020.109640.

References

Alatalo, D., Hassanipour, F., 2016. An experimental study on human milk viscosity. In: ASME 2016 International Mechanical Engineering Congress and Exposition, American Society of Mechanical Engineers. pp. V007T09A094–V007T09A094.

Alatalo, D., Jiang, L., Geddes, D., Hassanipour, F., 2020. Nipple deformation and peripheral pressure on the areola during breastfeeding. J. Biomech. Eng. 142.

Azarnoosh, J., Hassanipour, F., 2019. Effects of the non-newtonian viscosity of milk flow in the breast ductal system. In: ASME 2019 International Mechanical Engineering Congress and Exposition, American Society of Mechanical Engineers Digital Collection.

Azarnoosh, J., Sreenivas, K., Arabshahi, A., 2020. Numerical simulation of tidal breathing through the human respiratory tract. J. Biomech. Eng. https://doi.org/10.1115/1.4046005. In press.

Basch, K., 1893. Beiträge zur kenntniss des menschlichen milchapparats. Arch. Gynecol. Obstet. 44, 15–54.

Baum, K.G., McNamara, K., Helguera, M., 2008. Design of a multiple component geometric breast phantom. In: Medical Imaging 2008: Physics of Medical Imaging. International Society for Optics and Photonics, p. 69134H.

Bowen-Jones, A., Thompson, C., Drewett, R., 1982. Milk flow and sucking rates during breast-feeding. Dev. Med. Child Neurol. 24, 626–633.

Cheng, S., Gandevia, S., Green, M., Sinkus, R., Bilston, L., 2011. Viscoelastic properties of the tongue and soft palate using mr elastography. J. Biomech. 44, 450–454.

Drewe, C.J., Parker, L.P., Kelsey, L.J., Norman, P.E., Powell, J.T., Doyle, B.J., 2017. Haemodynamics and stresses in abdominal aortic aneurysms: a fluid-structure interaction study into the effect of proximal neck and iliac bifurcation angle. J. Biomech. 60, 150–156.

Elad, D., Kozlovsky, P., Blum, O., Laine, A.F., Po, M.J., Botzer, E., Dollberg, S., Zelicovich, M., Sira, L.B., 2014. Biomechanics of milk extraction during breast-feeding. Proc. Nat. Acad. Sci. 111, 5230–5235.

Geddes, D.T., 2007. Inside the lactating breast: the latest anatomy research. J. Midwifery Women's Health 52, 556–563.

Geddes, D.T., Kent, J.C., Mitoulas, L.R., Hartmann, P.E., 2008. Tongue movement and intra-oral vacuum in breastfeeding infants. Early Hum. Dev. 84, 471–477.

Gemci, T., Ponyavin, V., Chen, Y., Chen, H., Collins, R., 2008. Computational model of airflow in upper 17 generations of human respiratory tract. J. Biomech. 41, 2047–2054.

Imai, Y., Miki, T., Ishikawa, T., Aoki, T., Yamaguchi, T., 2012. Deposition of micrometer particles in pulmonary airways during inhalation and breath holding. J. Biomech. 45, 1809–1815.

King, M., Corden, J., David, T., Fisher, J., 1996. A three-dimensional, time-dependent analysis of flow through a bileaflet mechanical heart valve: comparison of experimental and numerical results. J. Biomech. 29, 609–618.

Kron, R., Litt, M., 1971. Fluid mechanics of nutritive sucking behaviour: the suckling infant's oral apparatus analysed as a hydraulic pump. Med. Biol. Eng. 9, 45–60.

Kurtcuoglu, V., Soellinger, M., Summers, P., Boomsma, K., Poulikakos, D., Boesiger, P., Ventikos, Y., 2007. Computational investigation of subject-specific cerebrospinal fluid flow in the third ventricle and aqueduct of sylvius. J. Biomech. 40, 1235–1245.

Li, W.Y., Gakwaya, S., Saey, D., Sériès, F., 2017. Assessment of tongue mechanical properties using different contraction tasks. J. Appl. Physiol. 123, 116–125.
Moore, S., David, T., Chase, J., Arnold, J., Fink, J., 2006. 3d models of blood flow in the cerebral vasculature. J. Biomech. 39, 1454–1463.
Mortazavi, S.N., Geddes, D., Hassanipour, F., 2017. Lactation in the human breast from a fluid dynamics point of view. J. Biomech. Eng. 139, 011009.
Mortazavi, S.N., Hassiotou, F., Geddes, D., Hassanipour, F., 2015. Mathematical modeling of mammary ducts in lactating human females. J. Biomech. Eng. 137, 071009.
Nobili, M., Morbiducci, U., Ponzini, R., Del Gaudio, C., Balducci, A., Grigioni, M., Montevecchi, F.M., Redaelli, A., 2008. Numerical simulation of the dynamics of a bileaflet prosthetic heart valve using a fluid–structure interaction approach. J. Biomech. 41, 2539–2550.
Patankar, S., 1980. Numerical Heat Transfer and Fluid Flow. CRC Press.
Pfaundler, M.v., 1899. Über saugen und verdauen. Wien. klin. Wschr 41, 1012.
Samani, A., Plewes, D., 2004. A method to measure the hyperelastic parameters of ex vivo breast tissue samples. Phys. Med. Biol. 49, 4395.
Tse, K.M., Chiu, P., Lee, H.P., Ho, P., 2011. Investigation of hemodynamics in the development of dissecting aneurysm within patient-specific dissecting aneurismal aortas using computational fluid dynamics (CFD) simulations. J. Biomech. 44, 827–836.
Valen-Sendstad, K., Mardal, K.A., Steinman, D.A., 2013. High-resolution CFD detects high-frequency velocity fluctuations in bifurcation, but not sidewall, aneurysms. J. Biomech. 46, 402–407.
Zoppou, C., Barry, S., Mercer, G., 1997. Dynamics of human milk extraction: a comparative study of breast feeding and breast pumping. Bull. Math. Biol. 59, 953–973.